Research Article

Abdi Ismail, Buana Ma'ruf*, Achmad Zubaydi*, Made Ayu Dwi Octavanny, and Turnad Lenggo Ginta

Strength assessment of fiberglass layer configurations in FRP ship materials from yard practices using a statistical approach

https://doi.org/10.1515/cls-2024-0007
received November 12, 2023; accepted April 11, 2024

Abstract: Fiberglass Reinforced Polymer (FRP) is a type of composite extensively used in small boats in Indonesia. Most FRP research focuses on general applications and research on FRP materials is not aligned with actual yard practices in lamination. This study examined the mechanical characteristics of marine-grade FRP composites applied to ships, considering fiberglass layer configurations that conform to yard practices and their compliance analysis with several international classification rules. Samples from Bojonegara and Makassar 3 met the criteria of the Indonesian Classification Bureau, Korean Register, and American Bureau of Shipping rules for tensile and bending strength and have the best specific strength. Analysis of Variance showed that the differences in fiberglass layer configurations had a significant impact on tensile and bending strength. Grouping using Tukey Simultaneous Tests indicated that samples with four or five layers showed tensile and bending strength that were not significantly different statistically. The Unsaturated Polyester Resin brand had a considerable impact on tensile strength but a less pronounced effect on bending strength. Sample Bojonegara and Makassar 3 can be recommended for practitioners in FRP shipyards as they have met the requirements of international regulations.

*** Corresponding author: Buana Ma'ruf,** Research Center for Hydrodynamic Technology, National Research and Innovation Agency, Surabaya, 60112, Indonesia, e-mail: buana.maruf@brin.go.id
*** Corresponding author: Achmad Zubaydi,** Department of Naval Architecture, Institut Teknologi Sepuluh Nopember, Surabaya, 60111, Indonesia, e-mail: zubaydi@na.its.ac.id
Abdi Ismail: Research Center for Hydrodynamic Technology, National Research and Innovation Agency, Surabaya, 60112, Indonesia
Made Ayu Dwi Octavanny: Department of Mathematics, Udayana University, Badung, 80361, Indonesia
Turnad Lenggo Ginta: Research Center for Industrial Process and Manufacturing Technology, National Research and Innovation Agency, Tangerang Selatan, 15312, Indonesia

Keywords: ship materials, lamination arrangement, FRP composite, mechanical properties, ANOVA

1 Introduction

Composite materials have been widely used in the maritime field. These materials are employed in various applications, ranging from small boats, recreational boats, fishing vessels, and offshore structures to renewable energy structures [1–5]. Composites can also be utilized for specific ship elements, such as superstructures, deck elements, bulkheads, propulsion system elements, and piping. Additionally, they find applications in offshore gas installations and underwater repairs [6].

Fiber Reinforced Polymer (FRP) is one of the alternative composite materials widely used in small boats in Indonesia [7]. These materials are known for their ease of fabrication, flexible geometry and shape, good material durability, corrosion resistance, and a high strength-to-weight ratio [8]. FRP materials require less significant investment compared to aluminum boats. Furthermore, they are lightweight, have straightforward technology, and do not demand highly skilled labor [9].

The majority of research on FRP composites applied for general applications focuses on matrix development, fibers, chemical agents, and the mechanical characteristics of these materials. There has been extensive research in developing Unsaturated Polyester Resin (UPR) for FRP composites, focusing on creating bio-based thermoplastic resins [10–12]. Studies on the thermoset capabilities of these resins have also been explored [13–15]. Additionally, research has addressed the incorporation of dynamic agents [16–19] and chemical depolymerization processes [20,21]. Substitution of synthetic and natural fibers has also been examined [22–25]. Investigations have been carried out on the fire resistance and adhesion of FRP for general applications [26–28]. The dynamic properties of FRP concerning impact, vibration, and material fatigue [29–31] have been studied. Furthermore, the mechanical strength characteristics of FRP have been researched [32–34].

Research on FRP composites applied to the shipbuilding industry has not been widely explored. Research on FRP materials with applications in building architecture has been conducted [10,35,36]. Applications in railways [37], tidal turbines [38], and the use of FRP for underwater pipe repairs [39] have also been discussed. Studies on the strength of FRP materials in Pleasure Craft Decks have been carried out, but the focus of this research was on sandwich structure combinations [40], which may not align with the practices used in Indonesian shipyards.

Furthermore, research on the mechanical characteristics of marine-grade FRP composites with UPR-fiberglass applied to ships and their compliance analysis with several international rules is still limited. However, regulations for FRP ship materials require the use of UPR and marine-grade fiberglass [41]. On the other hand, the effect of fiberglass layer configurations that conform to Indonesian yard practices on the strength of FRP ship materials has not been extensively studied.

Therefore, studying the influence of fiberglass layer configurations based on yard practices on the mechanical strength of marine-grade FRP ship materials is essential. This research is expected to serve as a reference for shipyards when manufacturing FRP ships with measurable material quality. Tensile and bending strength of FRP composites with various fiberglass layer configurations must be ensured to comply with the relevant regulations. The study will be conducted using samples produced by each shipyard following the yard practices of FRP shipyards in Indonesia. This is crucial to ensure that the tested samples accurately represent the actual lamination characteristics of each FRP shipyard. A statistical approach and specific strength analysis will be employed to compare which shipyard's lamination provides the most optimal mechanical strength for ship materials.

2 Material and method

This experimental research intends to evaluate the tensile and bending capabilities of marine-grade Chopped Strand Mat (CSM)–Woven Roving (WR) composites in comparison. Section 2 outlines the materials utilized for specimen preparation and the techniques employed for conducting uniaxial tensile and three-point flexure tests, which serve to address the stated research goal.

2.1 FRP ship materials

In this study, FRP composites were developed for the side shell plate of a ship's hull using marine-grade UPR. The research samples were fabricated using the hand-layup technique based on yard practices, with each sample being produced by different FRP shipyards. All samples were collected from experienced FRP shipyards in Indonesia, which met the Indonesian Classification Bureau (BKI) standards. The Indonesian Classification Bureau's standards are recognized internationally and refer to other international classification bodies. Each shipyard used marine-grade UPR with different brands and fiberglass layer configurations, as shown in Table 1. The table also provides an overview of the yard practices of various FRP shipyards in Indonesia. The FRP material specifications in this study were intentionally chosen based on Table 1 to evaluate how well the shipyard's practices align with the strength criteria defined by the rules. Furthermore, the use of sample specifications from yard practices in this research aims to represent the shipyard's practices better and to provide shipyard professionals with greater confidence in adopting samples that have been proven to meet the strength criteria of the rules.

Table 2 presents the types of resin used at these shipyards and their respective material characteristics. UPR A

Table 1: Shipyard lamination sample specification

No	Sample	Fiberglass layer configurations	UPR brand
1	Sample 1 (Banyuwangi)	CSM300, WR600, CSM600, WR600, CSM 450	UPR A
2	Sample 2 (Samarinda)	CSM300, CSM450, CSM450, WR800, CSM 450	UPR B
3	Sample 3 (Batam)	CSM300, WR900, CSM450, WR900	UPR C
4	Sample 4 (Tanjung Pinang)	CSM450, CSM800, CSM450, CSM800	UPR B
5	Sample 5 (Makassar 1)	CSM450, WR800, CSM450, WR800, CSM 450	UPR D
6	Sample 6 (Bojonegara)	CSM300, WR800, CSM450, WR800, CSM 450	UPR A
7	Sample 7 (Makassar 2)	CSM450, WR800, CSM450, WR800, CSM 450	UPR A
8	Sample 8 (Makassar 3)	CSM450, WR800, CSM450, WR800, CSM 450	UPR E

Table 2: Material characteristics of marine grade UPR brand A, B, C, D, and E

Properties	UPR A	UPR B	UPR C	UPR D	UPR E
Specific gravity (g/cm^3)	1.10 ± 0.02	1.14	1.16	1.1–1.2	1.0–1.12
Water Absorption (%)	0.188	0.24	0.4	0.18	0.17
Viscosity (cP)	450–500	300–400	650	540	30–40
Acid Value KOH (mg/g)	7–13	8–14	5	24.9	15–25
Gelling Time (min)	60	40	180–240	21	20–30

was supplied by PT. Justus Sakti Raya, Indonesia, UPR B and UPR C were purchased from Wee Tee Tong Chemicals Pte Ltd, and UPR D and UPR E were obtained from PT. Arindo Pacific Chemicals, Indonesia. The fiberglass used at each shipyard was a combat fiberglass consisting of CSM and WR. Methyl Ethyl Ketone Peroxide, used as a curing agent, was purchased from PT. Kawaguchi Kimia Indonesia and added an amount of 0.5% by weight of the resin to accelerate the hardening process during fiber lamination. The number of layers used varied from four to five layers in the eight shipyards.

The types of fiberglass mats and fiberglass rovings used include CSM with weights of 300, 450, 600, and 800 g/m^2, and WR with weights of 600, 800, and 900 g/m^2. Mat consists of filaments or continuous strands, or it can be in the form of pieces with a minimum length of 50 mm and is randomly oriented [42]. On the other hand, WR is a type of material used in the fiberglass ship lamination process, in woven form. WR layers are typically used on the inner layers, beneath the Mat layers, to ensure optimal resin absorption.

2.2 Experimental testing procedures

An experimental study was conducted to investigate tensile, bending, and specific strength in 8 FRP shipyards. The tensile and bending strength of the FRP ship material will be evaluated for compliance with the minimum requirements of the Indonesian Classification Bureau, Korean Register (KR), and the American Bureau of Shipping (ABS) [43,44]. Each shipyard was asked to create specimen sheets using the hand-lay-up technique, as shown in Table 1.

Uniaxial tensile tests and three-point bending tests were conducted using a calibrated Universal Testing Machine (RME 100 Schenck Trebel), as seen in Figure 1. Uniaxial tensile tests and three-point bending tests were performed on each sample until failure occurred. This allowed the determination of tensile strength (MPa) and bending strength (MPa) for each sample based on the maximum load that could be achieved [33]. Six specimens were required for each of these tests.

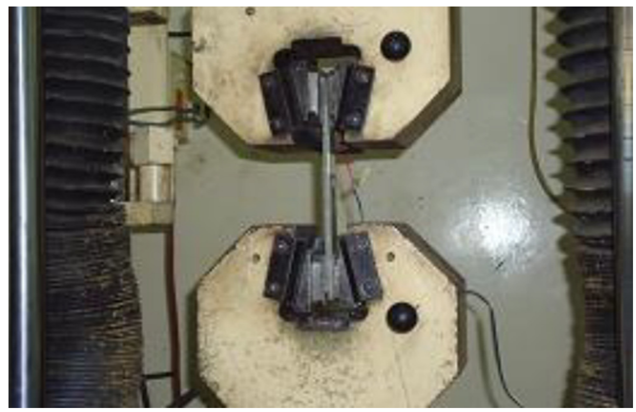

Figure 1: Tensile testing using a calibrated Universal Testing Machine.

The uniaxial tensile test was performed following ISO 527-3 (as suggested by the Indonesian Classification Bureau) at a crosshead speed of 5 mm/min [45]. Uniaxial tensile test specimens were fabricated in sheet form and cut to the dimensions of specimen type 3 in ISO 527-3, as shown in Figure 2(a)–(c). Uniaxial tensile test specimens had an overall length ($L3$) of 250 mm, width ($b1$) of 25 mm, and thickness (h) of 8 mm. Subsequently, tensile test data were reported as the average of 6 specimens with standard errors.

Three-point bending test specimens were also fabricated in sheet form and cut to the dimensions required by ISO 14125 (as suggested by the Indonesian Classification Bureau). Three-point bending test specimens had a specimen length (l) of 80 mm, an outer span (L) of 66 mm, width (b) of 15 mm, thickness (h) of 4 mm, the radius of central loading ($R1$) of 5 mm, and the radius of support members ($R2$) of 5 mm, as shown in Figure 3(a) and (b). Three-point bending tests were conducted with a strain rate of 0.01 (*i.e.*, 1% per minute) [46], and bending test data were reported as the average of six specimens with standard errors.

2.3 Specific strength calculation

Strength calculation of materials is based on the volume fraction of fibers and matrix as well as the direction of the

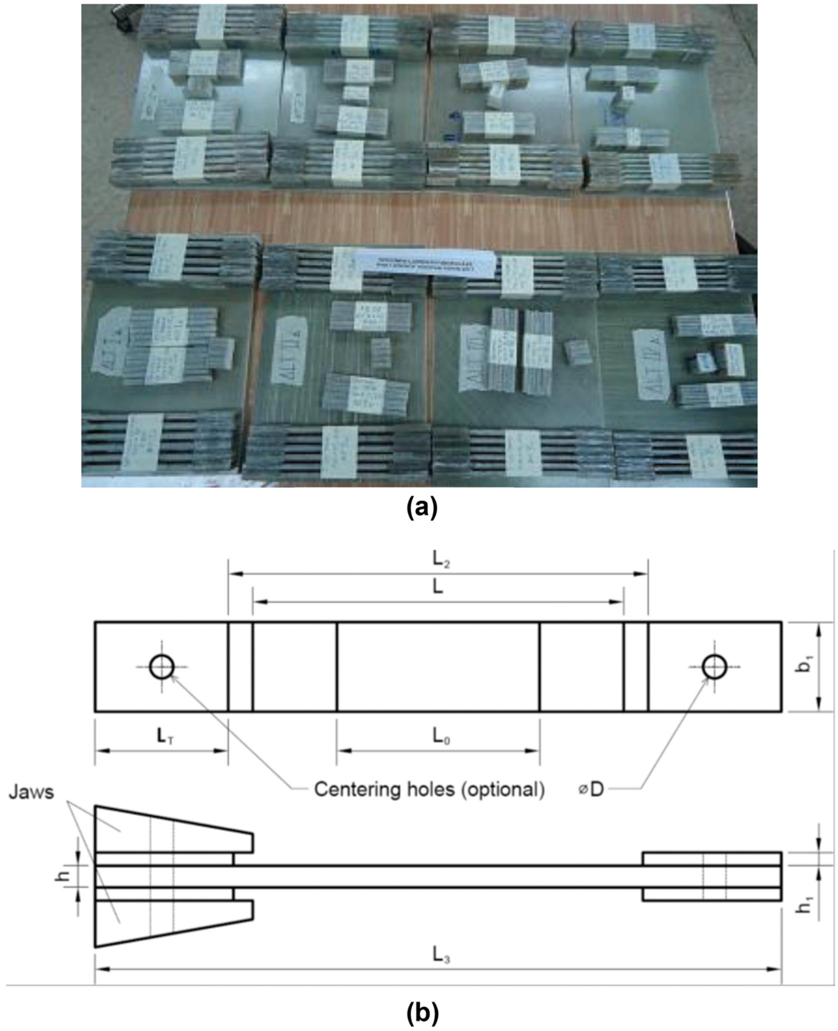

Figure 2: (a) Tensile and bending specimens. (b) Dimensions of the tensile test specimen.

fibers, the strain in the fiber, matrix, and the composite itself.

2.3.1 Rule of mixtures

The mechanical characteristics of composite materials are significantly influenced by the proportion of reinforcement and the matrix. Fundamental properties can be estimated by applying the rule-of-mixture principle under specific assumptions. The kind of reinforcement (whether it is fibers, particles, or whiskers) and their alignment are pivotal factors in establishing the composites' strength. In composite materials, when fibers are positioned at an angle, their strength in the direction of the fibers exceeds that in other orientations. Composite structure is also determined by its volume fraction of fiber and matrix. Furthermore, the volume of the composite can be calculated as follows:

Volume fraction of fiber:

$$V_f = \frac{v_f}{v_c}, \tag{1}$$

Volume fraction of matrix:

$$V_m = \frac{v_m}{v_c} \tag{2}$$

where v_f is the volume of fiber, and v_m is the volume of matrix.

Hence, volume of composite:

$$V_c = V_f + V_m. \tag{3}$$

Many researchers have highlighted that the fiber volume fraction stands as a primary parameter for ascertaining the mechanical characteristics of composites. Therefore,

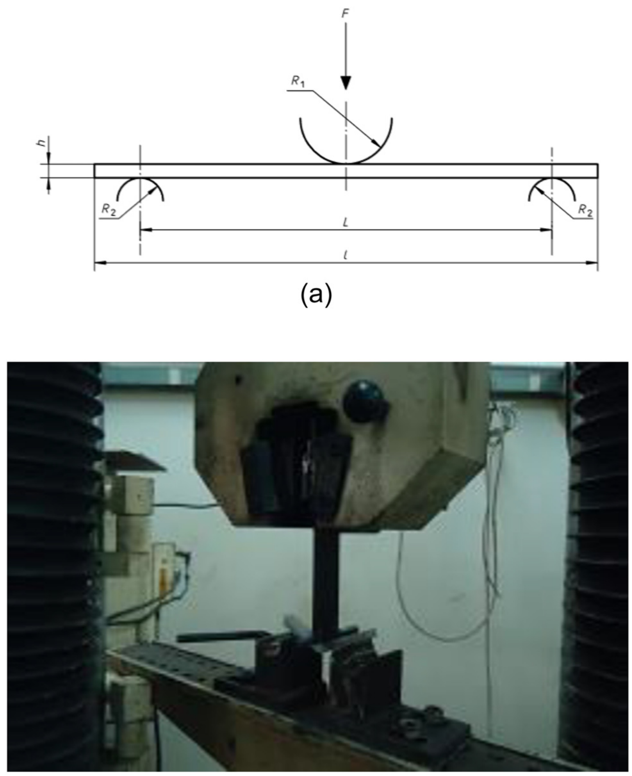

Figure 3: (a) Dimensions of the bending test specimen. (b) Bending testing.

it becomes essential to precisely establish this value. Typically, the fiber volume fraction is computed following the guidelines outlined in ASTM D2584 [47]:

$$V_{\mathrm{f}} = \frac{\rho_{\mathrm{m}}\omega_{\mathrm{f}}}{(\rho_{\mathrm{m}}\omega_{\mathrm{f}} + \rho_{\mathrm{f}}\omega_{\mathrm{m}})}, \tag{4}$$

where V_{f} is the volume fraction of fibers, W_{f} is the weight of fibers, and W_{m} is the weight of matrix, ρ_{f} is the density of fibers, and ρ_{m} is the density of matrix.

For unit volume of composite:

$$1 = V_{\mathrm{f}} + V_{\mathrm{m}}, \tag{5}$$

Volume fraction of matrix:

$$V_{\mathrm{m}} = 1 - V_{\mathrm{f}}. \tag{6}$$

Notations used in rule-of-mixture are as follows:

c, f, m represent composite, fiber, and matrix, respectively; V is the volume fraction, P is the load withstand, A is the cross-sectional area, E is the elastic modulus, σ is stress, ε is strain, μ is Poisson's ratio, and ρ is the density.

The density was determined through a displacement method, where the volume of the specimens immersed in water was equivalent to the volume displaced in a graduated cylinder. The weight of the specimens was quantified using a digital scale. The weight percentage of fiber (and matrix) in a polymer composite matrix quantifies the proportion of additive material within the overall composite. The weight percentage of additives provides insights into the composite's composition. A higher percentage indicates a greater proportion of fiber, which can lead to improved specific properties.

However, an excessive fiber content might compromise the matrix's integrity. Proper calculation ensures that the desired properties are achieved for specific applications. During the manufacturing processes of composites, the weight of the fibers and matrix were measured properly. Furthermore, to calculate the weight percentage of filler/fiber in a polymer composite matrix, the following formula can be applied:

$$\text{Weight\% of fiber glass} = \frac{\text{Weight of fiberglass}}{\text{Weight of composite}} \times 100\%. \tag{7}$$

2.3.2 Strength of composites

In the case of a fiber-oriented composite being subjected to a load aligned with the longitudinal direction of the fibers, the strain in the fiber, matrix, and the composite itself is uniform and equal, often referred to as iso-strain [48]. For iso-strain condition,

$$\varepsilon_{\mathrm{c}} = \varepsilon_{\mathrm{f}} = \varepsilon_{\mathrm{m}}, \tag{8}$$

as load withstand by composite can be presented as

$$P_{\mathrm{c}} = P_{\mathrm{f}} + P_{\mathrm{m}}, \tag{9}$$

and load withstand can also be written as

$$\sigma_{\mathrm{c}}A_{\mathrm{c}} = \sigma_{\mathrm{f}}A_{\mathrm{f}} + \sigma_{\mathrm{m}}A_{\mathrm{m}}. \tag{10}$$

Then, the strength of the composite, elastic modulus, and the density of composite for longitudinal load can be expressed as follows:

Strength of the composite

$$\sigma_{\mathrm{c}} = \sigma_{\mathrm{f}}v_{\mathrm{f}} + \sigma_{\mathrm{m}}v_{\mathrm{m}}. \tag{11}$$

Longitudinal elastic modulus of composite

$$E_{\mathrm{cl}} = E_{\mathrm{f}}v_{\mathrm{f}} + E_{\mathrm{m}}v_{\mathrm{m}}. \tag{12}$$

And, the density of the composite,

$$\rho_{\mathrm{c}} = \rho_{\mathrm{f}}v_{\mathrm{f}} + \rho_{\mathrm{m}}v_{\mathrm{m}}. \tag{13}$$

2.4 Statistical approach

A statistical approach was developed to determine the significance of the influence of fiberglass layer configurations on the strength of ship FRP materials. There are several assumptions that need to be met when performing an Analysis of Variance (ANOVA): independent observations, normally distributed observations in each group, and equal population variances in each group or homoscedasticity [49]. Observations meet the assumption of independence because they consist of different material compositions and laminations. Based on the KS test for normality, a *P*-value >0.150 was obtained for both the tensile test and bending test. It can be concluded that the observations are normally distributed.

The homogeneity of variances test results indicate that the population variances are equal (*P*-value from Levene's test = 0.071 for the tensile test and *P*-value from Levene's test = 0.435 for the bending test). If this assumption is not met, one alternative that can be applied is the Welch test [50–54]. In this study, all assumptions have been met, allowing for the continuation of ANOVA for each response, including the Tensile and Bending Tests.

3 Result and discussion

This section outlines the findings and discourse concerning the impact of UPR type and laminate arrangement on standardized tensile and flexural strength based on various rules. A comprehensive examination contrasts the standardized tensile and flexural strength acquired in this investigation with outcomes from diverse sources.

3.1 Compliance with rules

Experimental testing was conducted to determine the compliance of the strength of FRP ship materials with three sets of rules: the Indonesian Classification Bureau (BKI), the KR, and the ABS. These three sets of rules specify minimum requirements for tensile and bending strength, with both the KR and the Indonesian Classification Bureau having the same minimum requirements, as shown in Table 3.

Table 4 presents the average and standard error values obtained from the uniaxial tensile tests for each sample. The standard error values range from 1.4 to 7.1 MPa, with an average standard error in tensile strength of 4.7 MPa. Standard error indicates the range of mechanical strength values for FRP ship materials, where higher standard error values suggest variations in material quality or less homogeneity within the composite. The average standard error in tensile strength achieved in this study is quite good, as other FRP composite studies have reported higher average standard errors in tensile tests [55,56]. The standard error in tensile strength is significantly influenced by the hand lay-up method [57–59]. However, even FRP composite materials with better fabrication techniques, such as vacuum-assisted film infusion, had standard error values of 7.88 MPa [56], which is not better than those in this study. Similar results were also found in epoxy/fiberglass mat composites fabricated using the vacuum-assisted resin transfer molding technique [60].

The average and standard error of the three-point bending test for each sample are shown in Table 5. This study's average standard error of bending strength was also relatively good, at 9.8 MPa. These results were better than other fiberglass composites in the literature [55,56].

Table 3: Minimum requirement in three rules

Mechanical properties	ABS (MPa)	KR (MPa)	BKI (MPa)
Tensile Strength	123	98	98
Flexural Strength	172	150	150

Table 4: The tensile strength for each sample

Group	No						
	Tensile strength (MPa)						
	I	II	III	IV	V	VI	Average
Sample 1	85	99	120	126	123	93	107.7 ± 7.1
Sample 2	49	74	67	79	91	92	75.3 ± 6.6
Sample 3	80	83	55	79	68	93	76.3 ± 5.4
Sample 4	119	126	130	125	130	112	123.7 ± 2.9
Sample 5	113	129	132	124	103	132	122.2 ± 4.8
Sample 6	159	174	197	156	184	175	174.2 ± 6.3
Sample 7	110	96	100	103	106	117	105.3 ± 3.1
Sample 8	144	151	153	152	148	153	150.2 ± 1.4

Table 5: Bending Strength in each sample

Group	No						
	Bending strength (MPa)						
	I	II	III	IV	V	VI	Average
Sample 1	124	141	155	153	132	154	143.2 ± 5.3
Sample 2	102	109	110	101	97	122	106.8 ± 3.6
Sample 3	280	253	335	276	316	265	287.5 ± 12.8
Sample 4	190	152	68	164	136	176	147.7 ± 17.7
Sample 5	203	171	175	213	230	205	199.5 ± 9.3
Sample 6	234	271	282	288	240	313	271.3 ± 12.3
Sample 7	217	186	163	186	180	218	191.7 ± 8.9
Sample 8	233	224	255	226	259	205	233.7 ± 8.3

Table 6: The acceptability of each sample

Class Group	Tensile			Bending			Three rules
	ABS	KR	BKI	ABS	KR	BKI	
Sample 1		✓	✓				
Sample 2							
Sample 3				✓	✓	✓	
Sample 4	✓	✓	✓				
Sample 5		✓	✓	✓	✓	✓	
Sample 6	✓	✓	✓	✓	✓	✓	✓
Sample 7		✓	✓	✓	✓	✓	
Sample 8	✓	✓	✓	✓	✓	✓	✓

UPR/WR fiberglass and UPR/unidirectional discontinuous fiberglass composites fabricated using the same technique as in this study, which is hand lay-up, have higher average standard errors in bending strength, at 12.9 and 11 MPa, respectively [61]. Therefore, overall, shipyards in Indonesia appear to be realistic in still using the hand lay-up technique, as it is simpler and more cost-effective. In fact, the hand lay-up technique is still used in yacht fabrication in Italian shipyards [40].

Table 6 shows the acceptability of each sample regarding the tensile and bending strength criteria from the three rules. Samples that met the tensile and bending strength criteria of KR and the Indonesian Classification Bureau (BKI) were samples 5, 6, 7, and 8. Meanwhile, samples 6 and 8 were the only ones meeting the ABS criteria. Unfortunately, sample 4 only met the tensile strength criteria of ABS, KR, and BKI but not the bending strength criteria. On the other hand, sample 3 only met the bending strength criteria of ABS, KR, and BKI but not the tensile strength criteria.

Samples 5, 7, and 8 had the same fiberglass layer configurations; the difference lay in the UPR brand. Interestingly, only sample 8 met the criteria of all three rules, while Samples 5 and 7 only met the criteria of KR and BKI. The significance of the UPR brand's influence, based on the sample grouping, will be further explained in Section 3.3. Therefore, the best fiberglass layer configuration that could be applied as FRP ship material with only 5 layers and met the criteria of the three rules was the configuration of Samples 6 and 8. Samples 5 and 7 were actually suitable for the use of FRP ship material in Indonesia because they met the requirements of the Indonesian Classification Bureau (BKI). Still, Samples 6 and 8 were more convincing because they met the criteria of the three rules. Furthermore, a safety factor of 90% can be applied [62]. If this safety factor was calculated, the tensile and bending strength of Sample 6 became 156.8 and 244.2 MPa, respectively. Meanwhile, the tensile and bending strength of Sample 8 became 135.2 and 210.3 MPa. Based on these results, Samples 6 and 8 still met the criteria of the three rules even when the safety factor was considered. In general, it can be concluded that Samples 6 and 8 had the best fiberglass layer configuration.

3.2 Specific strength

The average calculation of tensile strength and bending strength are clearly presented in Table 7. The data was taken from six test-pieces for each sample and then the average was taken. As the fiber contents are given, with the rules of the mixture of composite equations, the fiber volume of fractions, the matrix volume of fractions, and the density of the composite can be determined accordingly. The average specific strength was calculated by dividing the average tensile strength by the density produced. When analyzing composite structure, it is important to calculate the specific strength of the composite instead of the strength itself. The higher the specific strength, the better the structure with lower weight.

Table 7: Strength calculation for tensile and bending test

No	Material and Lamination Composition	Fiber content (wt%)	Average tensile strength (N/mm^2)	Average bending strength (N/mm^2)	Fiber volume fraction	Matrix volume fraction	Composite density (g/m^3)	Specific tensile strength (N m/g)	Specific bending strength (N m/g)
1	Sample 1	29.0	107.7	143.2	0.230	0.770	1.19	90.5	120.3
2	Sample 2	25.0	75.3	106.8	0.196	0.804	1.18	63.8	90.5
3	Sample 3	37.1	76.3	287.5	0.302	0.698	1.22	62.5	235.7
4	Sample 4	38.7	123.7	147.7	0.316	0.684	1.23	100.6	120.1
5	Sample 5	33.6	122.2	199.5	0.271	0.729	1.21	101.0	164.9
6	Sample 6	40.3	174.2	271.3	0.331	0.669	1.23	141.6	220.6
7	Sample 7	33	105.3	191.7	0.265	0.735	1.21	87.0	158.4
8	Sample 8	33	150.2	233.7	0.265	0.735	1.21	124.1	193.1

The tensile strength and bending strength data are clearly presented as a graph as shown in Figures 4 and 5, respectively. It is obvious that Sample 6 had the highest values for tensile and Sample 3 had the best arrangement for bending. Furthermore, it is also clearly shown that Sample 6 had a significant value for the bending test. It can be concluded that Sample 6 gave the best results for the tensile and bending test.

Uniquely, even though Sample 3 had the highest bending and specific bending strength, the tensile and specific tensile strength of Sample 3 was very low. This phenomenon was caused by debonding between fiberglass layers, which is commonly found in various composites and can reduce bending strength [63]. Debonding is also a key factor in determining bending strength in sandwich composites, and various studies have been conducted on damage/debonding identification [64–66].

3.3 Statistical approach

3.3.1 Tensile test

In the tensile test response, the ANOVA results are shown in Table 8 as follows. Based on Table 8, an F-value of 44.84 was obtained. When compared to $F_{(0.05,7,40)}$ = 2.249, it led to

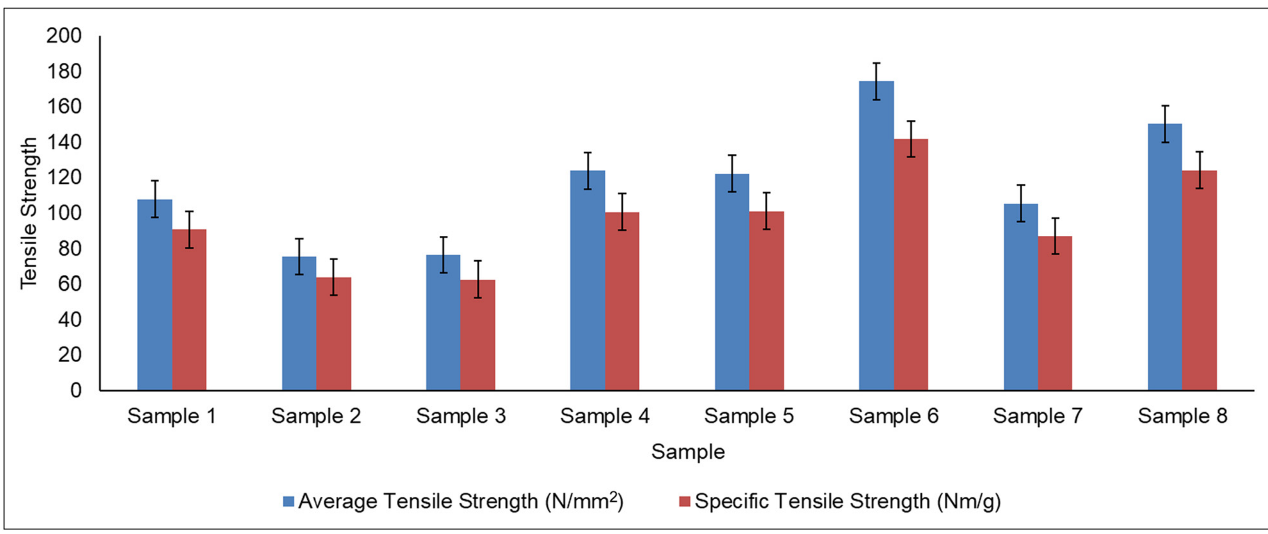

Figure 4: Average tensile strength and specific tensile strength.

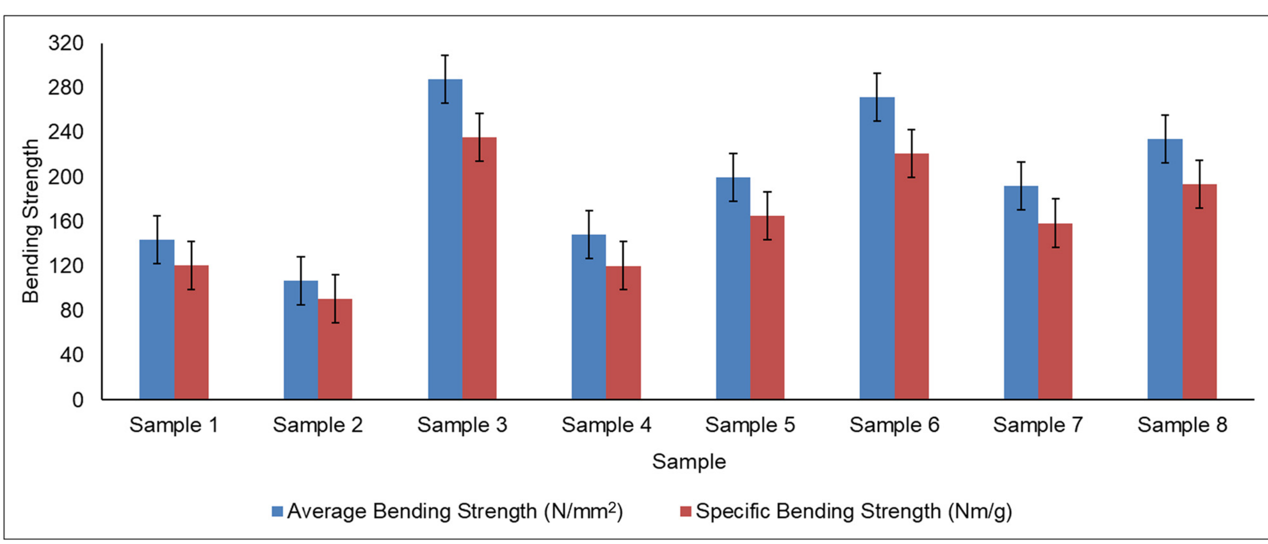

Figure 5: Average bending strength and specific bending strength.

Table 8: ANOVA of tensile test

Source	DF	Adj SS	Adj MS	*F*-Value	*P*-Value
Material and lamination composition	7	48,313	6901.8	44.84	0.000
Error	40	6,157	153.9		
Total	47	54,470			

the conclusion to reject the null hypothesis. Similarly, the *P*-value obtained was 0. When compared to $\alpha = 0.05$, the decision was made to reject the null hypothesis. It can be concluded that the difference in fiberglass layer configurations significantly affected the tensile test.

Figure 6 displays the interval plot of each material composition and lamination. It is evident that Sample 6, with fiberglass layer configurations CSM300 + 2 CSM450 + 2 WR800, achieved the highest result in the Tensile test when compared to other compositions. Although Sample 5, Sample 7, and Sample 8 shared the same fiberglass layer configurations (3 CSM450 + 2 WR800), they yielded different results due to variations in the UPR brand. The highest result was obtained by Sample 8, followed by Sample 5, and lastly, Sample 7. Once it was established that one or more fiberglass layer configurations had different means, the analysis proceeded with Tukey pairwise comparisons. The results of the simultaneous test for mean differences can be seen in Table 9 below.

Table 9 presents simultaneous tests for mean differences for all pairs with combinations of fiberglass layer configurations. The pairs of Sample 5 and Sample 1 had means that were not significantly different. The same applied to the pairs of Sample 7 and Sample 1, Sample 4 and Sample 1, Sample 2 and Sample 3, Sample 7 and Sample 5, Sample 4 and Sample 5, as well as Sample 4 and Sample 7. Based on the test results presented in Table 10, the following grouping can be established.

Table 10 provides information that Sample 6 with fiberglass layer configurations CSM300 + 2 CSM450 + 2 WR800 had the highest means and is in Group A. Sample 8 with the composition of 3 CSM450 + 2 WR800 was in Group B. Despite having the same fiberglass layer configurations, Sample 5 and Sample 7 were in Group C. The distinguishing factor between Samples 5, 7, and 8 was the UPR brand. This indicates that UPR E had a statistically significant effect on tensile strength because Sample 8 was categorized in a different group from Sample 5 and Sample 7. On the other hand, Sample 4 with fiberglass layer configurations 2 CSM450 + 2 CSM800 and Sample 1 with fiberglass layer configurations CSM300 + CSM450 + CSM600 + 2 WR600 are in Group C. Group D contained two members, namely Sample 3 and Sample 2.

Based on the grouping in Table 10, this indicates that the number of layers did not have a statistically significant impact on the results of the Tensile test. For example, Sample 4 with four layers, while Sample 5, Sample 1, and Sample 7 with five layers were in the same group. Similarly, Sample 3, which used four layers, was in the same group as Sample 2, which has five layers.

3.4 Bending test

In this section, the response to the Bending Test was also studied. Next, an ANOVA will be conducted with the results

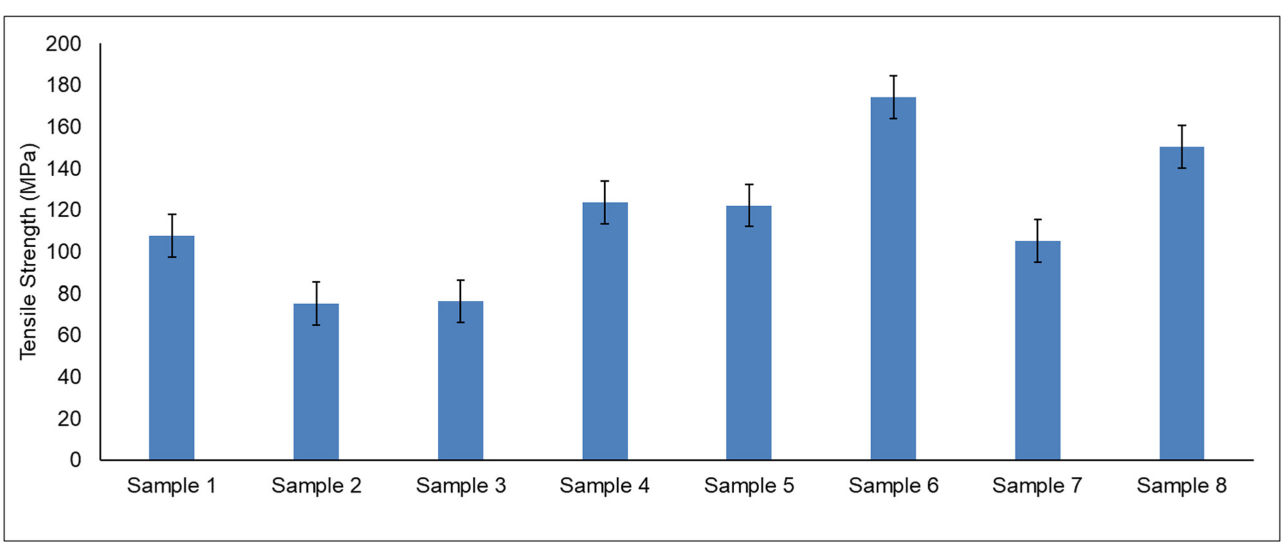

Figure 6: Interval plot of tensile test.

Table 9: Tukey simultaneous tests for differences of means of tensile test

Difference of Levels	Difference of means	*T*-Value	Adjusted *P*-Value
Sample 3–Sample 1	−31.33	−4.37	0.002
Sample 6–Sample 1	66.50	9.28	0.000
Sample 5–Sample 1	14.50	2.02	0.479*
Sample 7–Sample 1	−2.33	−0.33	1.000*
Sample 8–Sample 1	42.50	5.93	0.000
Sample 2–Sample 1	−32.33	−4.51	0.001
Sample 4–Sample 1	16.00	2.23	0.354*
Sample 6–Sample 3	97.83	13.66	0.000
Sample 5–Sample 3	45.83	6.40	0.000
Sample 7–Sample 3	29.00	4.05	0.005
Sample 8–Sample 3	73.83	10.31	0.000
Sample 2–Sample 3	−1.00	−0.14	1.000*
Sample 4–Sample 3	47.33	6.61	0.000
Sample 5–Sample 6	−52.00	−7.26	0.000
Sample 7–Sample 6	−68.83	−9.61	0.000
Sample 8–Sample 6	−24.00	−3.35	0.034
Sample 2–Sample 6	−98.83	−13.80	0.000
Sample 4–Sample 6	−50.50	−7.05	0.000
Sample 7–Sample 5	−16.83	−2.35	0.293*
Sample 8–Sample 5	28.00	3.91	0.008
Sample 2–Sample 5	−46.83	−6.54	0.000
Sample 4–Sample 5	1.50	0.21	1.000*
Sample 8–Sample 7	44.83	6.26	0.000
Sample 2–Sample 7	−30.00	−4.19	0.003
Sample 4–Sample 7	18.33	2.56	0.201*
Sample 2–Sample 8	−74.83	−10.45	0.000
Sample 4–Sample 8	−26.50	−3.70	0.014
Sample 4–Sample 2	48.33	6.75	0.000

Note: *indicated the corresponding means are not significantly different.

Table 10: Grouping Information Using the Tukey Method of Tensile Test

Rank	Sample	Fiberglass layer configurations	Mean	Grouping			
1	Sample 6	CSM300 + 2 CSM450 + 2 WR800	174.2	A			
2	Sample 8	3 CSM450 + 2 WR800	150.2		B		
3	Sample 4	2 CSM450 + 2 CSM800	123.7			C	
4	Sample 5	3 CSM450 + 2 WR800	122.2			C	
5	Sample 1	CSM300 + CSM450 + CSM600 + 2 WR600	107.7			C	
6	Sample 7	3 CSM450 + 2 WR800	105.3			C	
7	Sample 3	CSM300 + 2 WR900 + CSM450	76.3				D
8	Sample 2	CSM300 + 3 CSM450 + WR800	75.3				D

Note: Means that do not share a letter are significantly different.

Table 11: ANOVA of bending test

Source	DF	Adj SS	Adj MS	*F*-Value	*P*-Value
Material and lamination composition	7	171319	24474.1	36.17	0.000
Error	40	27066	676.7		
Total	47	198385			

shown in Table 11 as follows. Table 11 shows that the obtained *F*-value is 36.17. Similar to the tensile test, when compared with $F_{(0.05,7,40)} = 2.249$ it can be concluded that the null hypothesis was rejected. The same conclusion was reached when considering the *P*-value, which was 0. When compared with $\alpha = 0.05$ the decision was to reject the null hypothesis. It can be concluded that the differences in

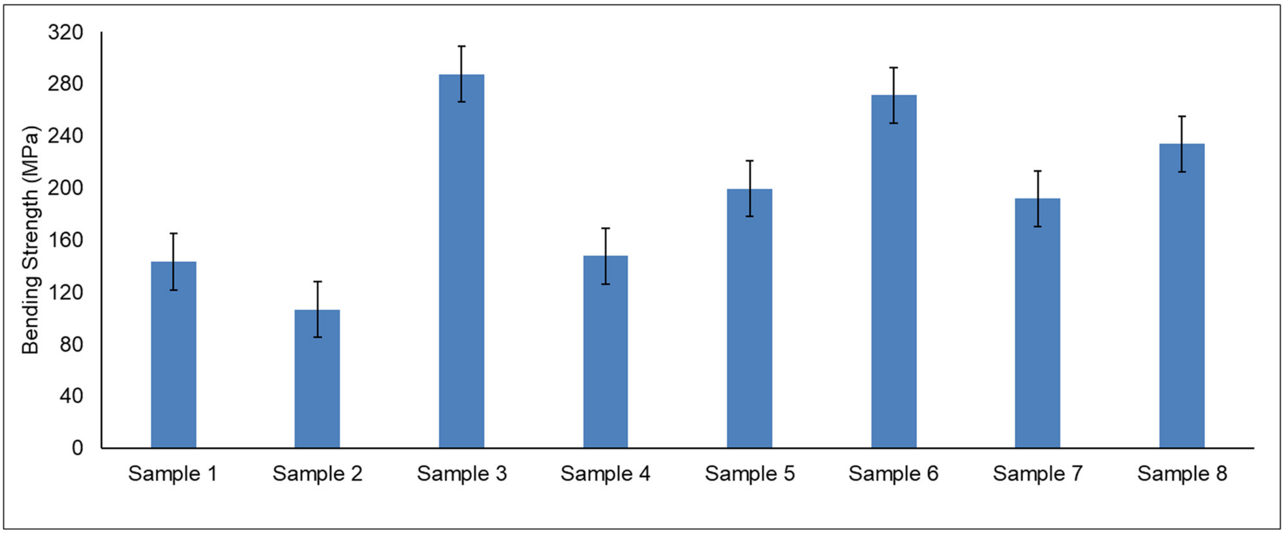

Figure 7: Interval Plot dari bending test.

fiberglass layer configurations had a significant impact on the bending test.

Figure 7 shows the interval plot for each material composition and lamination in the Bending Test. It can be seen that Sample 3, with the fiberglass layer configurations of CSM300 + 2 WR900 + CSM450, had the highest mean in the Bending test compared to other compositions. Following that, Sample 6, with fiberglass layer configurations of CSM300 + 2 CSM450 + 2 WR800, had the second-highest mean. Sample 2, with the lamination of CSM300 + 3 CSM450 + WR800, had the lowest mean. Figure 7 also indicates that each fiberglass layer configuration had a different mean. This aligns with the results of the *F*-test in the ANOVA (Table 11), which suggested that one or more fiberglass layer configurations had different means. Next, Tukey's pairwise comparison was conducted to further analyze the differences in mean for the Bending test. The results of the simultaneous test for mean differences in the Bending test are given in Table 12.

Using $\alpha = 0.05$, there were several pairs of fiberglass layer configurations that did not have significantly different means, as shown in Table 12. Sample 2 and Sample 1, Sample 4 and Sample 1, Sample 6 and Sample 3, and Sample 8 and Sample 6 did not have significantly different means. Similarly, for the pairs Sample 7 and Sample 5, Sample 8 and Sample 7, Sample 4 and Sample 7, and Sample 4 and Sample 2, there were no significant differences in means. Similar to the tensile test, based on the test results presented in Table 12, groupings can be made as shown in Table 13.

As shown in Table 13, Sample 3 with fiberglass layer configurations CSM300 + 2 WR900 + CSM450 fell into the same group (A) as Sample 6 (CSM300 + 2 CSM450 + 2 WR800). Even though they had a different number of layers, Samples 3 and 6 exhibited Bending test results that were not significantly different. Next, Sample 6 (CSM300 + 2 CSM450 + 2 WR800) was grouped with Sample 8 (3 CSM450 + 2 WR800) in Group B. The three fiberglass layer configurations from Samples 5, 7, and 8 were placed in the same group, which was Group C. Unlike the results of the Tensile test, these three compositions had Bending test results that were not significantly different.

Furthermore, Sample 7 (composition 3 CSM450 + 2 WR800) was grouped together with Sample 4 (composition 2 CSM450 + 2 CSM800) in Group D. Group E comprised three members: Sample 4 (composition 2 CSM450 + 2 CSM800), Sample 1 (composition CSM300 + CSM450 + CSM600 + 2 WR600), and Sample 2 (composition CSM300 + 3 CSM450 + WR800). This analysis was consistent with the previous analysis, which concluded that the number of layers did not significantly affect the mean bending strength. As in Group D, Sample 7 had five layers, and Sample 4 had four layers. In Group E, Sample 4 had four layers, while Sample 1 and Sample 2 had five layers.

Based on Tables 10 and 13, Samples 5, 7, and 8 exhibited the same trend in the order of the best tensile and bending strength values, which are, in sequence, Sample 8, Sample 5, and followed by Sample 7. These three samples shared the same fiberglass layer configurations, the only difference being the UPR brand used. Therefore, among the three UPR brands, the best ones, in sequence, were UPR E and UPR D, followed by UPR A. Moreover, statistically, Sample 8 (Group B) using UPR E demonstrated significantly higher tensile strength compared to Samples 5 and 7 in

Table 12: Tukey simultaneous tests for differences of means of bending test

Difference of Levels	Difference of means	*T*-Value	Adjusted *P*-value
Sample 3–Sample 1	144.3	9.61	0.000
Sample 6–Sample 1	128.2	8.53	0.000
Sample 5–Sample 1	56.3	3.75	0.012
Sample 7–Sample 1	48.5	3.23	0.046
Sample 8–Sample 1	90.5	6.03	0.000
Sample 2–Sample 1	−36.3	−2.42	0.260*
Sample 4–Sample 1	4.5	0.30	1.000*
Sample 6–Sample 3	−16.2	−1.08	0.958*
Sample 5–Sample 3	−88.0	−5.86	0.000
Sample 7–Sample 3	−95.8	−6.38	0.000
Sample 8–Sample 3	−53.8	−3.58	0.019
Sample 2–Sample 3	−180.7	−12.03	0.000
Sample 4–Sample 3	−139.8	−9.31	0.000
Sample 5–Sample 6	−71.8	−4.78	0.001
Sample 7–Sample 6	−79.7	−5.30	0.000
Sample 8–Sample 6	−37.7	−2.51	0.222*
Sample 2–Sample 6	−164.5	−10.95	0.000
Sample 4–Sample 6	−123.7	−8.23	0.000
Sample 7–Sample 5	−7.8	−0.52	0.999*
Sample 8–Sample 5	34.2	2.27	0.332*
Sample 2–Sample 5	−92.7	−6.17	0.000
Sample 4–Sample 5	−51.8	−3.45	0.026
Sample 8–Sample 7	42.0	2.80	0.125*
Sample 2–Sample 7	−84.8	−5.65	0.000
Sample 4–Sample 7	−44.0	−2.93	0.093*
Sample 2–Sample 8	−126.8	−8.45	0.000
Sample 4–Sample 8	−86.0	−5.73	0.000
Sample 4–Sample 2	40.8	2.72	0.147*

Note: * indicated the corresponding means are not significantly different.

Table 13: Grouping information using the tukey method of bending test

Sample	Fiberglass layer configurations	Mean	Grouping				
Sample 3	CSM300 + 2 WR900 + CSM450	287.5	A				
Sample 6	CSM300 + 2 CSM450 + 2 WR800	271.3	A	B			
Sample 8	3 CSM450 + 2 WR800	233.7		B	C		
Sample 5	3 CSM450 + 2 WR800	199.5			C		
Sample 7	3 CSM450 + 2 WR800	191.7			C	D	
Sample 4	2 CSM450 + 2 CSM800	147.7				D	E
Sample 1	CSM300 + CSM450 + CSM600 + 2 WR600	143.2					E
Sample 2	CSM300 + 3 CSM450 + WR800	106.83					E

Note: means that do not share a letter are significantly different.

Group C. It is important to note that differences in groups indicate significant differences in tensile strength.

In Table 13, it can be observed that Group A intersects with Group B, while Group B intersects with Group C. On the other hand, according to the bending test criteria for FRP ship materials set by the Indonesian Classification Bureau and KR, the material must have a bending strength greater than 150 MPa. Therefore, only Groups A, B, and C met these criteria. Notably, all the samples in Groups A, B, and C consist of at least two layers of woven fiberglass mat with a minimum weight of 800 g/m^2, which translates to two layers of WR 800 and two layers of WR 900. This indicates that an efficient fiberglass layer configuration for the side-shell of FRP ships should include at least two layers of WR 800 to meet the bending strength requirements. While using three layers or more of WR 800 or WR 900 is possible, such an approach might not be as efficient.

The CV for the Tensile test was 10.62%, and for the Bending test, it was 13.16%. These results are superior to the CV values in the tensile test for composite materials such as PU, PU resin, and Phenolic resin [67], as well as the CV in bending tests for composite beams under BS 5950 [68]. This research can serve as a reference for practitioners in FRP shipyards, indicating that to ensure compliance with the requirements for international classification rules regarding tensile and bending strength in the side-shell of FRP ships, fiberglass layer configurations like those in Samples 6 and 8 can be effectively applied in shipyard practices.

In the future, research on the lifetime of FRP ship materials needs to be further elaborated. The structural lifetime is highly determined by the dynamic characteristics of the ship due to wave loads, where wave spectra are commonly developed statistically. Additionally, the maximum side hull stresses also affect structural lifetime, and these are often studied using the Finite Element Method [69]. The development of vibration-based damage detection for FRP ship materials [70], where damage parameters are studied using a statistical approach, is also an interesting area to explore.

4 Conclusion

FRP is a composite material commonly used in small boats, recreational boats, and fishing vessels. Shipyards in developing countries like Indonesia often overlook the scientific aspects when designing fiberglass layer configurations for FRP boats. This study focused on assessing the strength of various fiberglass layer configurations based on different yard practices.

The coefficient of variations and standard errors of tensile and bending strength for the six specimens in the eight FRP samples show relatively good values compared to several references. Therefore, FRP fabrication using the hand lay-up technique is still recommended due to the reasonably good specimen results and cost-effectiveness. Samples 5, 6, 7, and 8 meet the tensile and bending strength criteria of the KR and the Indonesian Classification Bureau (BKI). However, only Samples 6 and 8 meet the tensile and bending strength criteria of the ABS. Thus, the fiberglass layer configurations of Samples 6 and 8 are recommended for use as the lamination arrangement for the hull of FRP boats. Another variable studied is specific strength, indicating samples with high strength and low weight. Specific strength analysis reveals that Samples 6 and 8 have the best specific tensile and specific bending strength.

A statistical approach was developed to assess the significance of tensile and bending strength among the samples. ANOVA results show that fiberglass layer configurations significantly affect the tensile and bending strength values. Furthermore, Tukey Simultaneous Tests were developed to group samples with specific ranges of tensile and bending strength values. Grouping using this method indicates that samples with four or five layers show tensile and bending strength values that are close or not significantly different statistically. The UPR brand considerably impacts tensile strength but has a less pronounced effect on bending strength. Fiberglass layer configurations in Samples 6 and 8 have significantly different tensile strength but not significantly different bending strength. Sample 3 has significantly higher bending strength than Sample 8, as shown by the group differences, but it has very low tensile strength in Group D and does not meet all rule criteria. Therefore, it can be concluded that the optimal fiberglass layer configurations recommended for implementation as hull lamination for FRP boats are the configurations from Samples 6 and 8.

Funding information: This research was funded by LPDP (Indonesia Endowment Funds for Education) through the Riset dan Inovasi untuk Indonesia Maju (RIIM) batch 3 program, managed by BRIN (National Research and Innovation Agency) under contract numbers B-839/II.7.5/FR.06/5/2023 and B-1066/III.3/FR.06/5/2023. The first author (Abdi Ismail) is a postdoctoral fellow under BRIN with contract number 151/II/HK/2022 dated September 1, 2022.

Author contributions: All authors have accepted responsibility for the entire content of this manuscript and consented to its submission to the journal, reviewed all the results and approved the final version of the manuscript. AI and BM contributed equally as the main contributor of this article. AI: investigation, formal analysis, writing – original draft, visualization; BM: conceptualization, methodology, resources, writing – review and editing; AZ: validation, data curation; MADO: formal analysis and statistical analysis; TLG: theory and analytic calculations.

Conflict of interest: The authors state no conflict of interest.

References

[1] Setvati MR, Shafiq N, Mustaffa Z, Syed ZI. A review on composite materials for offshore structures. In Proceedings of the International Conference on Offshore Mechanics and Arctic Engineering; 2014. p. 1–8.

[2] Cuadra J, Vanniamparambil PA, Hazeli K, Bartoli I, Kontsos A. Data-fusion progressive damage quantification in composites. In: Sano T, Srivatsan TS, Peretti MW, editors. The minerals, metals & materials society (TMS). San Diego: Springer; 2014. p. 137–44.

[3] Mouritz AP, Gellert E, Burchill P, Challis K. Review of advanced composite structures for naval ships and submarines. Compos Struct. 2001;53(1):21–42.

[4] Shenoi RA, Dulieu-Barton JM, Quinn S, Blake JIR, Boyd SW. Composite materials for marine applications: Key challenges for the future. In: Composite Materials. London: Springer-Verlag London; 2011. p. 69–89.

[5] Vizentin, G, Vukelic, G. Failure analysis of FRP composites exposed to real marine environment. In: Procedia Structural Integrity. Amsterdam: Elsevier; 2022. p. 233–40

[6] Rubino F, Nisticò A, Tucci F, Carlone P. Marine application of fiber reinforced composites: A review. J Mar Sci Eng. 2020;8(1):26.

[7] Zhang K, Zhang Q, Xiao J. Durability of FRP bars and FRP bar reinforced seawater sea sand concrete structures in marine environments. Constr Build Mater. 2022;350(39):128898.

[8] Jayaram S, Sivaprasad K, Nandakumar CG. Recycling of FRP boats. Int J Adv Res Eng Technol. 2018;9(3):244–52.

[9] Ma'ruf B, Ismail A, Purnama Sari D, Sujiatanti SH. Strength analysis of marine biaxial warp-knitted glass fabrics as composite laminations for ship material. Curved Layer Struct. 2023;10(1):20220209.

[10] Harmsen PFH, Hackmann MM, Bos HL. Green building blocks for bio-based plastics. Biofuels Bioprod Bioref. 2014;8(3):306–24.

[11] Rosenboom JG, Langer R, Traverso G. Bioplastics for a circular economy. Nat Rev Mater. 2022;7(2):117–37.

[12] Gandini A, Lacerda TM. From monomers to polymers from renewable resources: Recent advances. Prog Polym Sci. 2015;48(9):1–39.

[13] Shieh P, Zhang W, Husted KEL, Kristufek SL, Xiong B, Lundberg DJ, et al. Cleavable comonomers enable degradable, recyclable thermoset plastics. Nature. 2020;583(7817):542–7.

[14] Wang B, Wang X, Xu N, Shen Y, Lu F, Liu Y, et al. Recycling of carbon fibers from unsaturated polyester composites via a hydrolysis-oxidation synergistic catalytic strategy. Compos Sci Technol. 2021;203(3):108589.

[15] Di Mauro C, Genua A, Rymarczyk M, Dobbels C, Malburet S, Graillot A, et al. Chemical and mechanical reprocessed resins and bio-composites based on five epoxidized vegetable oils thermosets reinforced with flax fibers or PLA woven. Compos Sci Technol. 2021;205(5):108678.

[16] Memon H, Wei Y, Zhu C. Recyclable and reformable epoxy resins based on dynamic covalent bonds – Present, past, and future. Polym Test. 2022;105(1):107420.

[17] Aranberri I, Landa M, Elorza E, Salaberria AM, Rekondo A. Thermoformable and recyclable CFRP pultruded profile manufactured from an epoxy vitrimer. Polym Test. 2021;93(1):106931.

[18] Hayashi M. Versatile functionalization of polymeric soft materials by implanting various types of dynamic cross-links. Polym J. 2021;53(7):779–88.

[19] Yang X, Guo L, Xu X, Shang S, Liu H. A fully bio-based epoxy vitrimer: Self-healing, triple-shape memory and reprocessing triggered by dynamic covalent bond exchange. Mater Des. 2020;186(2):108248.

[20] Navarro CA, Ma Y, Michael KH, Breunig HM, Nutt SR, Williams TJ. Catalytic, aerobic depolymerization of epoxy thermoset composites. Green Chem. 2021;23(17):6356–60.

[21] Kim DH, Yu A, Goh M. Oxidative chemical depolymerization of thermoset epoxy resin for green recycling. J Ind Eng Chem. 2021;96(4):76–81.

[22] Faruk O, Bledzki AK, Fink HP, Sain M. Biocomposites reinforced with natural fibers: 2000–2010. Prog Polym Sci. 2012;37(11):1552–96.

[23] Staiger, MP, Tucker, N. Natural-fibre composites in structural applications. In Properties and performance of natural-fibre composites. Amsterdam: Elsevier Inc; 2008. p. 269–300.

[24] Lau KT, Hung PY, Zhu MH, Hui D. Properties of natural fibre composites for structural engineering applications. Compos Part B Eng. 2018;136(5):222–33.

[25] Wambua P, Ivens J, Verpoest I. Natural fibres: Can they replace glass in fibre reinforced plastics? Compos Sci Technol. 2003;63(9):1259–64.

[26] Mayya HB, Pai D, Kini VM, Padmaraj NH. Effect of marine environmental conditions on physical and mechanical properties of fiber-reinforced composites – A review. J Inst Eng Ser C. 2021;102(3):843–9.

[27] Etcheverry M, Barbosa SE. Glass fiber reinforced polypropylene mechanical properties enhancement by adhesion improvement. Mater (Basel). 2012;5(6):1084–113.

[28] Zhang S, Chu F, Xu Z, Zhou Y, Hu W, Hu Y. Interfacial flame retardant unsaturated polyester composites with simultaneously improved fire safety and mechanical properties. Chem Eng J. 2021;426(27):131313.

[29] Santos FM, Temarel P, Guedes Soares C. Modal analysis of a fast patrol boat made of composite material. Ocean Eng. 2009;36(2):179–92.

[30] Liu C, Wu X, Gao X. Comparisons of tension–tension fatigue behavior between the 3D orthogonal woven and biaxial warp-knitted composites. J Text Inst. 2021;112(8):1249–57.

[31] Putić S, Stamenović M, Bajčeta B, Stajčić P, Bošnjak S. The influence of high and low temperatures on the impact properties of glass-epoxy composites. J Serbian Chem Soc. 2007;72(7):713–22.

[32] Kopparthy SDS, Netravali AN. Review: Green composites for structural applications. Compos Part C Open Access. 2021;6(3):100169.

[33] Belingardi G, Paolino DS, Koricho EG. Investigation of influence of tab types on tensile strength of E-glass/epoxy fiber reinforced composite materials. In: Procedia Engineering. Amsterdam: Elsevier; 2011. p. 3279–84

[34] Singh AP, Yadav A, Mishra S, Khan KLA, Gupta A. Effect of metallic fillers on mechanical properties of FRP composite. In: Lecture Notes in Mechanical Engineering. Berlin: Springer Science and Business Media; 2021. p. 615–24

[35] Smits J. Fiber-reinforced polymer bridge design in the Netherlands: Architectural challenges toward innovative, sustainable, and durable bridges. Engineering. 2016;2(4):518–27.

[36] Lucherelli MA, Duval A, Avérous L. Biobased vitrimers: Towards sustainable and adaptable performing polymer materials. Prog Polym Sci. 2022;127(4):101515.

[37] Ito M, Nagai K. Degradation issues of polymer materials used in railway field. Polym Degrad Stab. 2008;93(10):1723–35.

[38] Hantoro R, Utama IKAP, Arief IS, Ismail A, Manggala SW. Innovation in vertical axis hydrokinetic turbine – Straight blade cascaded (VAHT-SBC) design and testing for low current speed power generation. J Phys Conf Ser. 2018;1022(1):012023.

[39] Shamsuddoha M, Islam MM, Aravinthan T, Manalo A, Lau KT. Effectiveness of using fibre-reinforced polymer composites for underwater steel pipeline repairs. Compos Struct. 2013;100(6):40–54.

[40] Di Bella G, Galtieri G, Borsellino C. Three-point flexural properties of bonded reinforcement elements for pleasure craft decks. Appl Compos Mater. 2018;25(1):21–34.

[41] Biro Klasifikasi Indonesia. Rules for fibreglass reinforced plastic ships, rules for classification and construction. Jakarta, Indonesia: Biro Klasifikasi Indonesia; 2006.

[42] Suresh Barthe S, Dadalal Rathod Y, Gaikar AA, Dhagate VK. Overview of hand layup FRP molding process. Int J Adv Res Sci Commun Technol (IJARSCT). 2022;2(2):373–7.

[43] Korean Register. Rules for the classification of FRP ships. Korean Register; 2014.
[44] American Bureau of Shipping. Rules for building and classing reinforced plastic vessels. ABS; 1978.
[45] ISO 527-3. Plastics – determination of tensile properties – part 3: test conditions for films and sheets. Geneva, Switzerland: ISO Committee; 2018.
[46] ISO 14125. Fibre-reinforced plastic composites – determination of flexural properties. Geneva, Switzerland: ISO Committee; 1998.
[47] Messiry MEl. Theoretical analysis of natural fiber volume fraction of reinforced composites. Alex Eng J. 2013;52(3):301–6.
[48] Chung DDL. Composite materials. 2nd edn. Derby B, editor. New York: Springer; 2010.
[49] Ostertagová E, Ostertag O. Methodology and application of oneway ANOVA. Am J Mech Eng. 2013;1(7):256–61.
[50] Welch BL. On the comparison of several mean values: An alternative approach. Biometrika. 1951;38(3):330.
[51] Nguyen D, Pham TV, Kim E, Chen YH, Wang Y, Kromrey JD. Empirical comparison of tests for one-factor ANOVA under heterogeneity and non-normality: A Monte Carlo study. J Mod Appl Stat Methods. 2019;18(2):2–30.
[52] Liu H. Comparing Welch's ANOVA, a Kruskal-Wallis test and traditional ANOVA in case of Heterogeneity of Variance. Richmond: VCU Scholars Compass Theses; 2015.
[53] Delacre M, Leys C, Mora YL, Lakens D. Taking parametric assumptions seriously: arguments for the use of Welch's F-test instead of the classical F-test in one-way ANOVA. Int Rev Soc Psychol. 2019;32(1):1–12.
[54] Holliday NM. Flagellation testing of composite finger skirts for surface effect ship (SES) application. Melbourne: Florida Tech; 2021.
[55] Gao X, Li D, Wu W, Chen S. Experimental investigation of the tensile and bending behavior of multi-axial warp-knitted fabric composites. Text Res J. 2018;88(3):333–44.
[56] Chen J, Gao X, Zhao K, Wu W. Research on influence of matrix component on the mechanical behavior of multiaxial warp-knitted composites. Fibers Polym. 2022;23(11):3126–37.
[57] Gljušćić M, Franulović M, Lanc D, Božić Ž. Digital image correlation of additively manufactured CFRTP composite systems in static tensile testing. Procedia Struct Integr. 2021;31(2019):116–21.
[58] Brčić M, Kršćanski S, Brnić J. Rotating bending fatigue analysis of printed specimens from assorted polymer materials. Polym (Basel). 2021;13(7):1–11.
[59] Vizentin G, Vukelic G. Prediction of the deterioration of FRP composite properties induced by marine environments. J Mar Sci Eng. 2022;10(4):1–11.
[60] Mohamed M, Selim MM, Ning H, Pillay S. Effect of fiber prestressing on mechanical properties of glass fiber epoxy composites manufactured by vacuum-assisted resin transfer molding. J Reinf Plast Compos. 2020;39(1–2):21–30.
[61] Jariwala H, Jain P, Maisuriya V. Experimental and statistical analysis of strength of glass fiber reinforced polymer composite for different fiber architecture. Polym Compos. 2021;42(3):1407–19.
[62] Molkens T, Cashell KA, Rossi B. Post-fire mechanical properties of carbon steel and safety factors for the reinstatement of steel structures. Eng Struct. 2021;234(1):111975.
[63] Pan Z, Wu Z, Xiong J. Localized temperature rise as a novel indication in damage and failure behavior of biaxial non-crimp fabric reinforced polymer composite subjected to impulsive compression. Aerosp Sci Technol. 2020;103(8):105885.
[64] Tuswan T, Zubaydi A, Piscesa B, Ismail A, Ariesta RC, Prabowo AR. A numerical evaluation on nonlinear dynamic response of sandwich plates with partially rectangular skin/core debonding. Curved Layer Struct. 2022;9(1):25–39.
[65] Ariesta RC, Tuswan T, Zubaydi A, Ismail A. Identification of damage size effect of natural frequency on sandwich material using free vibration analysis. NAŠE MORE Znan časopis za more i Pomor. 2022;69(1):1–8.
[66] Ismail A, Zubaydi A, Piscesa B, Tuswan T. A novel fiberglass-reinforced polyurethane elastomer as the core sandwich material of the ship-plate system. J Mech Behav Mater. 2023;32(1):1–14.
[67] Milanese AC, Cioffi MOH, Jacobus H, Voorwald C. Mechanical behavior of natural fiber composites. In: Procedia Engineering. Amsterdam: Elsevier; 2011. p. 2022–7.
[68] Liu J, Ding FX, Liu XM, Yu ZW, Tan Z, Huang JW. Flexural capacity of steel-concrete composite beams under hogging moment. Adv Civ Eng. 2019;2019(1):1–13.
[69] Ismail A, Zubaydi A, Piscesa B, Tuswan T, Ariesta RC. Study Of sandwich panel application on side hull of crude oil tanker. J Appl Eng Sci. 2021;19(4):1090–8.
[70] Ismail A, Zubaydi A, Piscesa B, Ariesta RC, Tuswan T. Vibration-based damage identification for ship sandwich plate using finite element method. Open Eng. 2020;10(1):744–52.